Electronic Supplementary Material (ESI) for Physical Chemistry Chemical Physics.

Electronic Supplementary Information: The Transformation of Cuboctahedral to Icosahedral Nanoparticles: Atomic Structure and Dynamics

Philipp N. Plessow*

Institute of Catalysis Research and Technology (IKFT), Hermann-von-Helmholtz-Platz 1, 76344 Eggenstein-Leopoldshafen, Germany.

E-mail: plessow@kit.edu

S1 Parameterization of the Gupta potential for DFT structures

The parameters were optimized to reproduce structures obtained with DFT (PBE-D3) calculations. In particular, the fit was carried out for the icosahedral and cuboctahedral structures of the 147-atomic clusters. For Cu, Ag and Ni, the root-mean-squared (rms) deviation for the Cartesian coordinates of these structures with the parameters in Table S1 was below 0.03 Å. The structural fit was generally worst for the heavy elements Pt and Au with rms-deviations up to 0.09 Å. Eventually, the fitted Gupta potential was only used for the elements with relatively low barriers for transitions, Cu, Ag, Au and Ni. For the other elements, larger deviations between energies obtained from DFT constrained optimization and DFT single points were observed. The parameters in Table S1 were used for Cu_{561} and Cu_{923} in Fig. 1 and Fig. 2 and for Ag_{561}, Au_{561}, Ni_{309}, and Ni_{561} in Table 1 in the main text.

Table S1: Parameters for the Gupta potential optimized to reproduce DFT structures, determining the parameters up to the ratio A/x. The absolute value of A was for Cu fit to DFT barriers and for Ag and Ni taken from ref. 1.

Element	A (eV)	p	r_0 (Å)	x (eV)	q
Cu	0.1283	9.8340	2.5790	1.6965	2.5490
Ag	0.1028	9.5143	2.9173	1.3581	2.1889
Au	0.2061	9.0392	3.0207	3.0954	2.2825
Ni	0.0376	10.2817	2.4809	0.4690	2.7314

S2 Additional results with existing parameterizations of the Gupta potential

The parameters were taken from Table I in Ref. 1 for all metals considered in the main text (Cu, Ag, Au, Ni, Pd, Pt, Rh and Ir) and from Table I in Ref. 2 for the metals available: Cu, Ag, Au, Pd and Pt. Using these parameterizations, barriers for symmetric and asymmetric transformation from cuboctahedral to icosahedral structures were determined as discussed in the main text.

Overall, the parameterizations from both Ref. 1 and Ref. 2 behave similarly. The largest deviations are observed for Au and Pd, however, even here deviations are relatively small, less than 0.5 eV. The trends are largely as described in the main text for the DFT calculations. Barriers are ascending roughly in the order Cu, Ni, Ag, Au, Pd, Pt, Rh, Ir.

All transition states were optimized with a convergence criterion of 10^{-4} eV/Å for forces on individual atoms. Tight convergence thresholds are necessary due to the very low curvatures and the resulting low frequency vibrations. The imaginary frequencies for the transition mode are on the order of 10 cm^{-1}. All transition states were verified to have only a single imaginary frequency. The connectivity was furthermore checked through small displacements along the transition mode followed by optimizations that led to icosahedron and cuboctahedron, respectively. For Pt_{561} and Pd_{561}, we found for both parameterizations a flat region on the potential energy surface after the transition state, approximately 0.5 eV below the transition state. Conversion to the icosahedron requires to surmount an additional, extremely small barrier of less than 0.01 eV. It was not possible to determine the correct transition state for Pt_{561} with the parameterization in Ref. 1. Both parameterizations for Au lead to problematic geometry optimizations that did not allow to determine the precise transition state for Au_{309} and Au_{561}. For Cu_{147} both parameterization predict that the cuboctahedron is not a minimum but a first-order saddle point. Distortion along the transition mode leads to the two isomers of the icosahedron that can be accessed in the plus- or minus-direction of ξ. The obtained activation energies are given in Table S2 and the differences between symmetric and asymmetric energy barriers is listed in Table S3.

Using harmonic transition state theory, activation entropies S_a and activation free energies F_a were calculated. The activation entropies at $T = 300$ K are shown in Fig. S1 as a function of the activation barrier E_a. It can be seen that the activation entropy generally

increases with cluster size from 147-, over 309- to 561-atomic clusters. For a given cluster size, the entropy differs only little between different metals, although there is a tendency for metals with larger activation barriers to have also higher activation entropies.

Table S2: Activation energies E_a in eV for the cuboctahedral-to-icosahedral transformation (excluding zero point correction) obtained with the Gupta potential.

n	Cu	Ag	Au	Ni	Pd	Pt	Rh	Ir
147	$0.00^{a,b}$	0.50^{b}	1.14^{b}	0.02^{b}	1.27^{b}	1.99^{b}	1.74^{b}	4.05^{b}
309	0.66^{b}	2.06^{b}		1.08^{b}	3.55^{b}	5.02^{b}	6.65^{b}	11.70^{b}
561	2.80^{b}	4.64^{b}		4.37^{b}	7.28^{b}		14.85^{b}	24.19^{b}
147	$0.00^{a,c}$	0.50^{c}	1.23^{c}		1.35^{c}	1.87^{c}		
309	0.65^{c}	2.05^{c}			3.69^{c}	5.14^{c}		
561	2.75^{c}	4.62^{c}			7.23^{c}	10.06^{c}		

[a] The cuboctahedron of Cu_{147} is not a minimum, but a first-order saddle point.
[b] Gupta potential with parameterization from Ref. 1.
[c] Gupta potential with parameterization from Ref. 2.

Table S3: Difference between symmetric and asymmetric activation energy in eV. In case of a non-zero difference, the highest point of the symmetric transition is a higher-order saddle point on the potential energy surface.

n	Cu	Ag	Au	Ni	Pd	Pt	Rh	Ir
147	$0.00^{a,b}$	0.00^{b}	0.16^{b}	0.00^{b}	0.09^{b}	0.24^{b}	0.00^{b}	0.09^{b}
309	0.00^{b}	0.26^{b}		0.00^{b}	0.84^{b}	1.49^{b}	0.44^{b}	1.78^{b}
561	0.11^{b}	1.13^{b}		0.00^{b}	2.38^{b}		2.48^{b}	6.02^{b}
147	$0.00^{a,c}$	0.00^{c}	0.34^{c}		0.11^{c}	0.15^{c}		
309	0.00^{c}	0.27^{c}			0.90^{c}	1.28^{c}		
561	0.13^{c}	1.14^{c}			2.80^{c}	3.98^{c}		

[a] The cuboctahedron of Cu_{147} is not a minimum, but a first-order saddle point.
[b] Gupta potential with parameterization from Ref. 1.
[c] Gupta potential with parameterization from Ref. 2.

Activation free energies are shown in Fig. S2 as a function of temperature. The trend is the same as for the activation entropies at 300 K: The temperature-dependence increases with cluster size. Although the absolute effect of temperature is similar for different metals, the relative effect can differ significantly, because of the different magnitude of activation energies. For example, the energy barrier of Ag_{561} is 4.6 eV and that of Ir_{561} is 24.2 eV. The absolute decrease of the free energy barrier at $T = 500$ K is similar in both cases, on the

order of 2 to 3 eV. The relative decrease, however, is about 50% for Ag_{561}, while it is only around 10% for Ir_{561}.

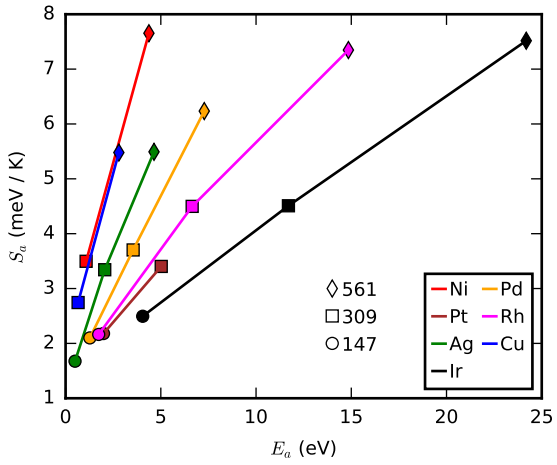

Figure S1: The activation entropy S_a is shown as a function of the activation barrier, both computed using the Gupta potential with the parameterization from Ref. 1 and harmonic TST.

Constrained MD simulations with umbrella integration were carried out as described in the main text, however, using only 22 trajectories at different values of ξ_0. The elements Au, Pt and Pd that led poor convergence in transition state optimizations also caused problems for some constrained MD simulations. The quality of the constrained MD simulations was judged based on the convergence of the free energy gradient $\mathrm{d}F/\mathrm{d}\xi$ with t, which was generally very good, and the smoothness of $\mathrm{d}F/\mathrm{d}\xi$ as a function of ξ. Based on the latter criterion, the simulations for Pt_{561} and Au_{309} at $T = 50$ K using the parameters from Ref. 2 were discarded.

As discussed in the main text, the collective variable ξ acts on the corner atoms to enforce the transformation. Alternatively, the force on the corner atoms may also act as an artificial driving force for diffusion of these atoms on the surface of the clusters. This is a problem mainly at high temperatures, when the atoms become mobile enough to leave their most stable positions. The occurrence of this phenomenon also depends on the barrier height of the cuboctahedral-to-icosahedral transition. For higher barriers, the force acting on the corner atoms is larger and so is the driving force for the atoms to diffuse over the surface. To generally prevent this, additional pairwise constraining potentials were applied based on two threshold d_1 and d_2. The constraints were applied between all pairs of atoms in the outer shell (atom 1) and all atoms in the outer or second shell (atom 2) if the distance d between atom 1 and 2 is smaller than d_1 both in the icosahedron and in the cuboctahedron. A quadratic attractive potential $k/2(d-d_2)^2$ with $k = 50$ eV/Å^2 was applied for these pairs for distances $d > d_2$. The distance d_1 was chosen to capture the nearest neighbor distance and d_2 was chosen larger, to not significantly perturb regular vibrations. This was checked by increasing d_2 by 10% (about 0.3 to 0.4 Å) for all 147- and 309-atomic clusters for 200 and 400 K. This led to a mean absolute deviation of 0.03 eV and a maximum deviation of 0.11

eV. The parameters are listed in Table S4.

Table S4: Values of the parameters d_1 and d_2 in Å.

n	Cu	Ag	Au	Ni	Pd	Pt	Rh	Ir
d_1	3.00	3.39	3.37	2.92	3.22	3.25	3.15	3.18
d_2	3.40	3.84	3.82	3.31	3.65	3.68	3.57	3.61

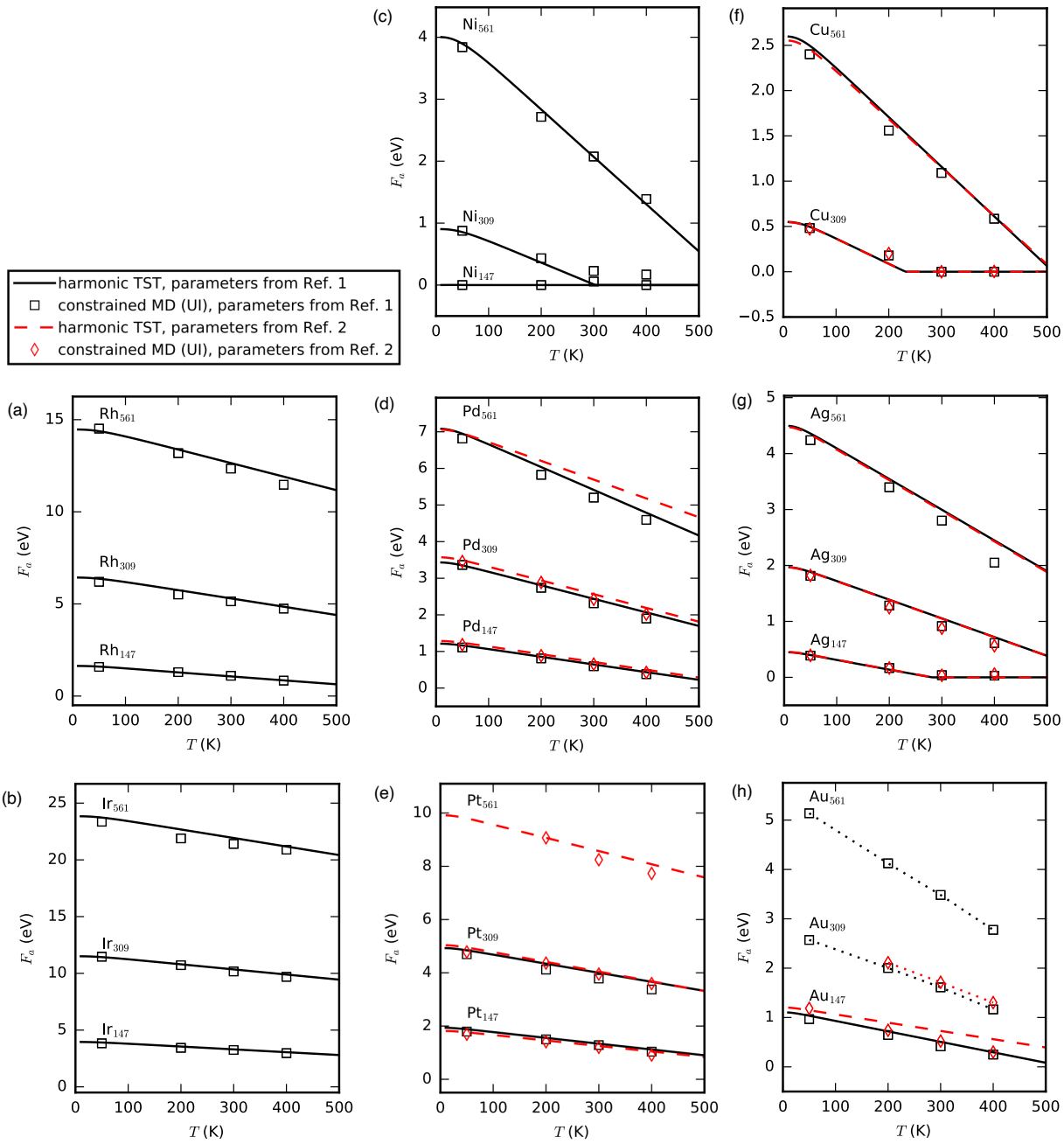

Figure S2: Cuboctahedral-to-icosahedral transition of clusters obtained with the Gupta potential using parameterization from Ref. 1 (black) and Ref. 2 (red). Results from harmonic transition state theory are shown as lines and results from constrained MD simulations (Umbrella Integration) as symbols. (a) Rh (b) Ir (c) Ni (d) Pd (e) Pt (f) Cu (g) Ag (h) Au. Additional dotted lines connect the data points from constrained MD for Au_{309} and Au_{561}, where transition states were not obtained.

S3 Results of NEB-calculations

Figure S3 shows the energies obtained with NEB-calculations that were used to computed the activation energies shown in Table 1 in the main text.

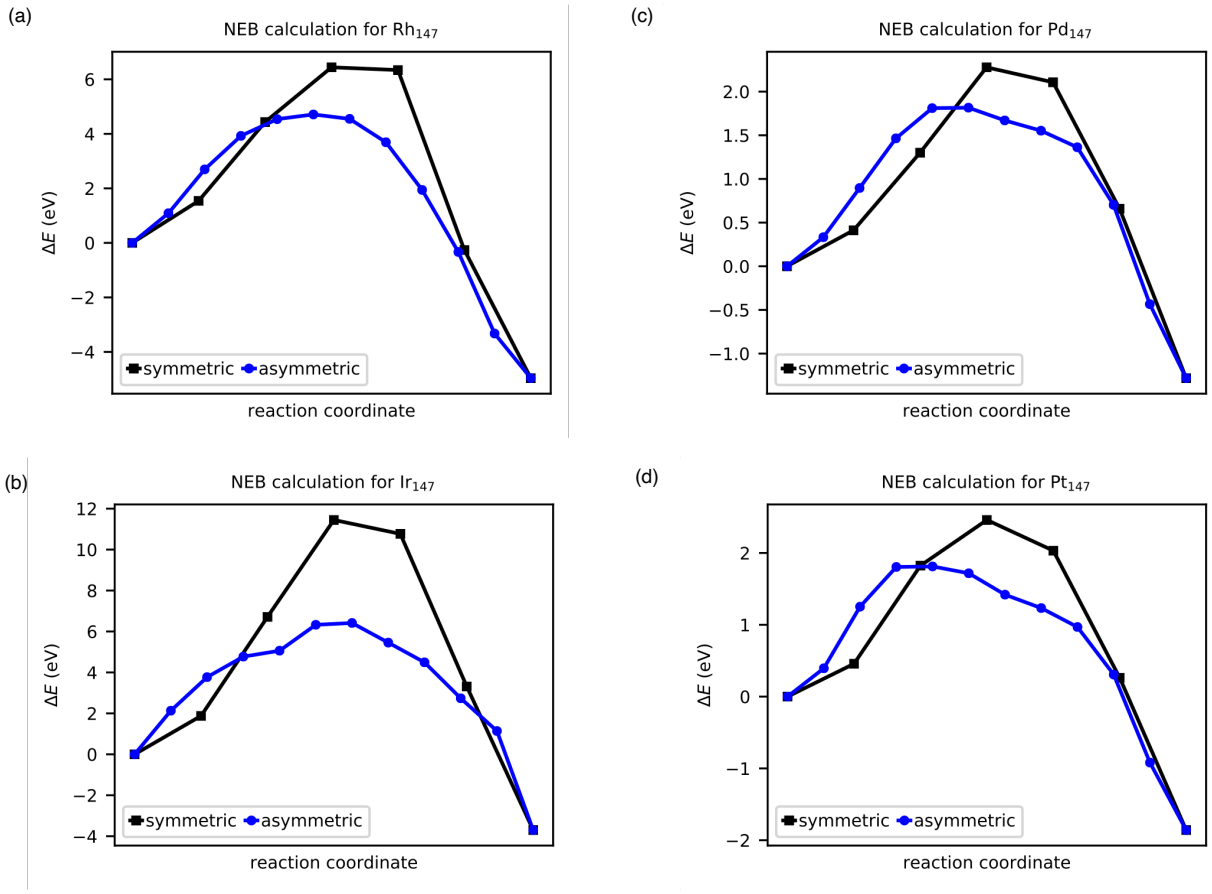

Figure S3: NEB calculations for the cuboctahedral-to-icosahedral transition of the 147-atomic nanoparticles of a) Rh, b) Ir, c) Pd and d) Pt. Energies are referenced to the cuboctahedron.

References

(1) Cleri, F.; Rosato, V. V. Tight-binding potentials for transition metals and alloys. *Phys. Rev. B* **1993**, *48*, 22–33.

(2) Baletto, F.; Rapallo, A.; Rossi, G.; Ferrando, R. Dynamical effects in the formation of magic cluster structures. *Phys. Rev. B* **2004**, *69*, 235421.